ACS APPLIED POLYMER MATERIALS

pubs.acs.org/acsapm

Article

Influence of Diallyl Disulfide on the Properties of Biobased Antimicrobial Vitrimers for Microimprint Lithography

Liepa Daugelaite, Sigita Grauzeliene, Danguole Bridziuviene, Vita Raudoniene, Egidija Rainosalo, and Jolita Ostrauskaite*

Cite This: https://doi.org/10.1021/acsapm.5c00412

Read Online

ACCESS | Metrics & More | Article Recommendations | Supporting Information

ABSTRACT: This work contributes to the development of sustainable materials by creating biobased photopolymerized vitrimers with antimicrobial, shape-memory, and self-welding capabilities, essential for industries using light-based manufacturing technologies where petroleum-based materials lacking such properties are currently used. In this study, the influence of the amount of diallyl disulfide, which has antimicrobial properties and forms dynamic bonds, on the vitrimeric behavior and antimicrobial activity of biobased vitrimers synthesized from acrylated epoxidized soybean oil, 2-hydroxy-3-phenoxypropyl acrylate, and diallyl disulfide was determined. The addition of 0.35 mol of diallyl disulfide to a resin containing 1 mol of acrylated epoxidized soybean oil and 1 mol of 2-hydroxy-3-phenoxypropyl acrylate was found to reduce resin viscosity by 55%, photocuring rate by 30% and shrinkage to 0%, and increase polymer flexibility by 53%. These polymers exhibited excellent self-welding and shape-memory properties enabled by dynamic disulfide bond exchange. Antimicrobial tests have shown that resins containing more than 0.05 mol of diallyl disulfide, 1 mol of acrylated epoxidized soybean oil, and 1 mol of 2-hydroxy-3-phenoxypropyl acrylate inhibit the bacterial growth of *Escherichia coli* by more than 97%, *Staphylococcus aureus* by more than 49%, as well as the fungal growth of *Aspergillus flavus* by more than 83%, and *Aspergillus niger* by more than 38% after 1 h of direct contact with the bacterial or fungal suspensions. Micrometer-scale patterns formed using microimprint lithography confirmed the potential of these vitrimers with diallyl disulfide moieties as antimicrobial advanced engineering materials for applications where flexibility and sustainability are required.

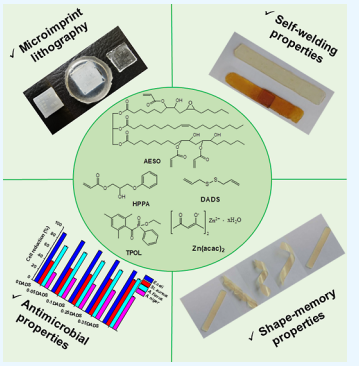

KEYWORDS: *vitrimer, diallyl disulfide, shape-memory, self-welding, reprocessing, antimicrobial, microimprint lithography*

1. INTRODUCTION

The antimicrobial properties of polymers are essential in various fields, as they contribute significantly to improving the safety, hygiene, and long service-life of the products.[1] For example, in healthcare, they help prevent infections by reducing microbial colonization and bacterial growth on medical devices.[2] Similarly, in the food industry and textile manufacturing, antimicrobial polymers are vital to maintain cleanliness and extend product shelf life.[3,4] Furthermore, antimicrobial plastics gained increased attention during the COVID-19 pandemic as a potential solution to curb the spread of infection through surface transmission by reducing the need for harmful chemical disinfectants.[5] However, despite their importance, many existing antimicrobial polymers are synthesized from petroleum-based starting materials, raising concerns about their environmental impact.[6,7] These polymers often lack properties such as shape-memory, self-welding, and reprocessability.[8,9] Solving this problem requires new ways to create sustainable materials with useful properties. In this context, vitrimers have become a novel class of materials that not only exhibit the durable and high-strength characteristics of thermosetting polymers, but also offer additional benefits, such as reprocessability and adaptability to adjust their shape and properties responding to external stimuli, particularly heat, which are crucial for creating advanced antimicrobial surfaces.[10−12]

Due to their dynamic covalent exchange reactions, such as disulfide bond exchange, vitrimers can maintain a stable network while exhibiting properties including shape-memory, self-welding, and reprocessability.[13−15] These characteristics do not directly confer antimicrobial activity, but make vitrimers a highly versatile platform for the development of next-generation antimicrobial materials. In order to support the development of versatile and environmentally sustainable materials, the objective of this work was to examine how diallyl disulfide incorporation affects the antimicrobial efficiency, mechanical strength, and vitrimeric properties of vitrimers. These materials aim to reduce microbial contamination while promoting environmental sustainability ultimately

Received: February 4, 2025
Revised: April 25, 2025
Accepted: April 25, 2025

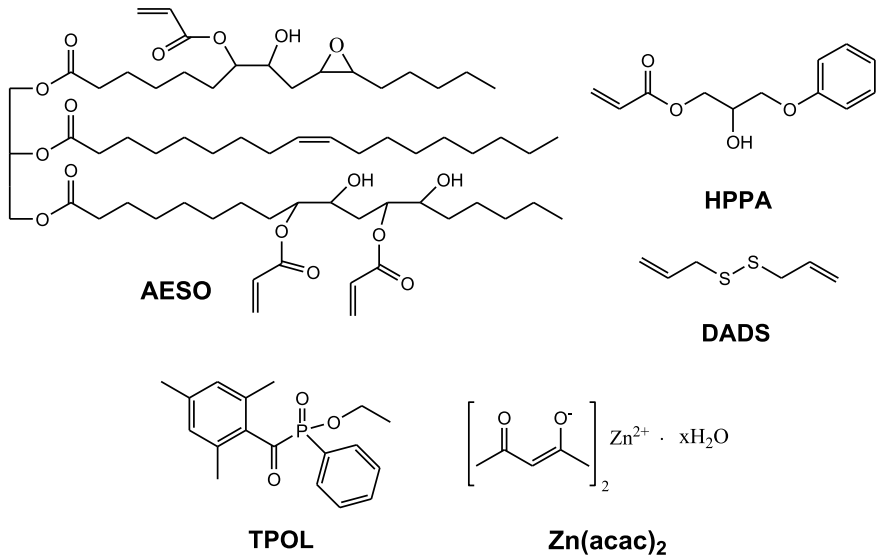

Figure 1. Chemical structures of acrylated epoxidized soybean oil (AESO), 2-hydroxy-3-phenoxypropyl acrylate (HPPA), diallyl disulfide (DADS), ethyl(2,4,6-trimethylbenzoyl)phenylphosphinate (TPOL), and zinc acetylacetonate hydrate ($Zn(acac)_2$).

offering safer and more durable solutions for a range of high-performance applications, e.g. formation of replicas by microimprint lithography that could be used in microelectronic devices, biosensors, and optical systems. Therefore, the selection of the biobased monomers was carefully considered to achieve antimicrobial efficacy of vitrimers. Acrylated epoxidized soybean oil (AESO) (Figure 1) was chosen as the monomer due to renewable nature as it is derived from a widely available agricultural resource, and ability to impart flexibility and rigidity due to a large number of functional groups (3 acrylic, 1 epoxy, 3 hydroxy groups and 1 carbon−carbon double bond per triglyceride) groups of the polymer network.[16−18] This selection is consistent with the increasing demand for biobased materials that minimize dependence on petrochemical resources. Furthermore, the incorporation of 2-hydroxy-3-phenoxypropyl acrylate (HPPA), known for its efficiency in transesterification reactions, further contributed to the dynamic properties and flexibility of the vitrimer.[19−21] HPPA reduces cross-linking density due to its lower functionality compared to AESO. In addition, it forms bulky side chains with aromatic rings, which prevent polymer chains from approaching each other closely. This steric hindrance creates free volume between the polymer chains and lowers the cross-linking density. As a result, the reduced cross-linking density leads to increased chain mobility and thus more flexible materials, despite the presence of rigid aromatic segments. Diallyl disulfide (DADS) was selected for its antimicrobial activity,[22] which enhances the ability of vitrimer to prevent microbial contamination. The antimicrobial activity of polymers with DADS fragments was not previously reported in the literature, making this study a novel contribution to the area of polymer research. The disulfide bonds incorporated into the polymer structure play an important role in the dynamic behavior of the vitrimer, allowing reversible bond exchange under specific conditions, such as heat or pH changes.[23] This dynamic exchange capability not only supports the reprocessability and self-welding properties of the material, but also ensures that the antimicrobial functionality is maintained throughout lifecycle of the material. DADS is a natural organosulfur compound that is found mostly in garlic and other *Allium* plants.[24] It contributes to the characteristic aroma and health benefits of garlic. DADS is highly valued in polymer science due to its ability to enhance the properties of polymers, particularly by improving their flexibility.[23] In addition, DADS demonstrates potent antimicrobial properties, proving effectiveness against a variety of viruses, fungi, and bacteria.[22] These properties make it a promising additive in the development of antimicrobial materials and coatings. As a photoinitiator, ethyl(2,4,6-trimethylbenzoyl)-phenylphosphinate (TPOL) was chosen due to its high reactivity and efficiency in generating free radicals under UV light, leading to fast cure and the formation of transparent products. Its low intrinsic color and clean photodecomposition contribute to the high clarity in the final product, making it ideal for applications requiring transparency and color stability.[25] As a transesterification catalyst, zinc acetylacetone hydrate ($Zn(acac)_2$) was chosen due to its high catalytic efficiency under mild conditions, which allows effective ester group exchange in polymer networks.[26] It is compatible with various polymer systems, making it a preferred choice in sustainable polymer chemistry. Additionally, microimprint lithography was used to create micrometer-scale features on a substrate by mechanically transferring patterns from a mold onto a surface. This method is a cost-effective alternative to traditional photolithography, enabling precise control over the shape and dimensions of the patterned structures, and is used in the fabrication of microelectronic devices and biosensors.[27] Incorporating DADS into polymers for microimprint lithography offers a solution to improve the flexibility and mechanical resilience of replicas, as its aliphatic structure allows the network to absorb stress more effectively and reduces crack formation in microstructures.

2. MATERIALS AND METHODS

2.1. Materials. Soybean oil epoxidized acrylate (AESO), 2-hydroxy-3-phenoxypropyl acrylate (HPPA), diallyl disulfide (DADS), and zinc acetylacetone hydrate ($Zn(acac)_2$) were purchased from Merck. Ethyl(2,4,6-trimethylbenzoyl)phenylphosphinate (TPOL) was obtained from Fluorochem. All chemicals were used without further purification.

https://doi.org/10.1021/acsapm.5c00412
ACS Appl. Polym. Mater. XXXX, XXX, XXX−XXX

Table 1. Composition of Resins

resin	amount of AESO (mol)	amount of HPPA (mol)	amount of DADS (mol)	amount of TPOL (mol %)	amount of $Zn(acac)_2$ (wt %)	viscosity (mPa·s)
0DADS	1	1	0	3	0	8475 ± 190
0.05DADS			0.05		0	7253 ± 90
0.1DADS			0.1		0	6807 ± 244
0.25DADS			0.25		0	5408 ± 200
0.35DADS			0.35		0	4703 ± 120
0.35DADS5Zn			0.35		5	[a]

[a]Not measured.

2.2. Preparation of UV/Vis-Curable Resins. The mixtures of starting materials were prepared using AESO, HPPA, DADS monomers, and the photoinitiator TPOL. A series of five samples were prepared without and with different amounts of DADS (Table 1). Additional sample with the highest amount of DADS was prepared using 5 wt % of the catalyst $Zn(acac)_2$. The amount of photinitiator[28] and catalyst[29,30] was used based on the previous research.

The mixtures were stirred at 40 °C until homogeneity was reached. They were poured into a (70 × 10 × 1) ± 0.01 mm Teflon mold and irradiated with a 500 W Helios Italquartz lamp, with a radiation intensity of 310 mW·cm^{-2} at 250−450 nm. The temperature reached 80 °C, which was maintained throughout the entire irradiation period. Photocuring was carried out for 7−10 min until a solid polymer formed.

The resin code is compiled as follows: the first number represents the amount of DADS in moles in the resin, DADS is allyl disulfide, the second number indicates the percentage concentration of the catalyst $Zn(acac)_2$ in the resin, Zn is zinc acetylacetonate hydrate.

2.3. Self-Welding Test. After photocuring, samples measuring (70 × 10 × 1) ± 0.01 mm were divided into two equal parts. One part of the sample was manually pressed against the other with sufficient force to ensure full contact along a length of 1 cm. Then these polymer samples were heated for 1 h at 180 °C and mechanically tested using a BDO-FB0.5TH (Zwick/Roell) device. Tensile testing was used to calculate the self-welding efficiency as the percentage ratio of tensile strength retained by the welded sample compared to the original (unwelded) material.

2.4. Shape-Memory Test. A shape memory test was conducted on a polymer sample measuring (70 × 10 × 1) ± 0.01 mm. The sample was twisted into a spiral shape using a glass rod. The twisted polymer sample was cooled to 5 °C. The time it took for the polymer sample to return to its original shape at room temperature was recorded.

2.5. Reprocessability Test. The reprocessability test of polymer samples was conducted using a CARVER (Carver Inc., Wabash, IN, USA) hot press. Polymer samples of (70 × 10 × 1) ± 0.01 mm were crushed into powder in the presence of liquid nitrogen, poured into a preheated stainless steel frame, compressed between two stainless steel heated to 210 °C hot press plates. The sample was heated for 25 min under a pressure of 4 t. After heating, the polymer sample was slowly (within 1 h) cooled under pressure to room temperature.

2.6. Antimicrobial Tests. The antimicrobial activity of the polymers was evaluated following a methodology adapted from prior research.[31] Microbial inoculum concentrations were prepared as follows: 1.75 × 10^6 colony forming units/mL (cfu/mL) for *Escherichia coli* (*E. coli*), 7.45 × 10^6 cfu/mL for *Staphylococcus aureus* (*S. aureus*), 3.85 × 10^5 cfu/mL for *Aspergillus flavus* (*A. flavus*), and 1.00 × 10^5 cfu/mL for *Aspergillus niger* (*A. niger*). A 10 μL suspension of bacteria or fungi was applied to the surface of the test films (dimensions 1 × 1 cm) and incubated under high humidity conditions (90% relative humidity) at 35 °C for bacterial strains and 26 °C for fungal strains for 1 h. The reduction in viable microorganisms was calculated according to the formula: [(initial cfu/mL − remaining cfu/mL)/initial cfu/mL] × 100%. Results were averaged from three independent experiments for consistency.

2.7. Microimprint Lithography. A 1951 USAF resolution test target structure was fabricated using an Asiga Pico2 39 UV 3D printer with PlasGray material. To produce a soft mold for replica fabrication, polydimethylsiloxane (PDMS) was cast over the printed structure and cured at 100 °C for 1 h. The resins were cured for 10 min using a 500 W Helios Italquartz GR.E UV lamp, which emitted of 250−450 nm light at intensity of 310 mW·cm^{-2}.

2.8. Characterization Techniques. The kinetics of photopolymerization and the rheological properties of the resins were investigated with an Anton Paar MCR302 rheometer containing a plate/plate accessory and an OmniCure S2000 irradiation device (Lumen Dynamics Group Inc.). The viscosity of the resins was measured across a shear rate range of 0.001−50 s^{-1}, at a temperature of 25 °C, for 60 s. Photocuring test was carried out with three repetitions over 150 s in shear mode, a frequency of 10 Hz, and UV/vis radiation was activated 30 s after the start of the test. During the experiment, the following parameters were recorded after 120 s of irradiation: storage modulus (G'), loss modulus (G''), layer shrinkage, and complex viscosity (η^*). The induction period was determined as the duration from the start of UV/vis irradiation to the beginning of the G' curve increase. The gel point (t_{gel}) was determined as the crossover point of the G' and G'' curves, and it was calculated from the start of irradiation.

The cross-linking density of the polymers was calculated using equation[32]

$$G' = \nu \cdot R \cdot T \quad (1)$$

where: G'—storage modulus value from the G' curves 120 s after the start of irradiation (Pa); ν—cross-linking density (mol/m^3); R—universal gas constant (J/mol K); T—temperature (K).

The chemical structure of the polymers was verified using Fourier transform infrared (FT-IR) spectroscopy. Spectrum BX II FT-IR spectrometer was used to record FT-IR spectra. The reflection of the polymer sample was measured. The wavenumber ranged from 650 to 4000 cm^{-1}.

IR reflection bands of polymers with DADS (cm^{-1}): 3461 (v, O−H), 2928 (v, CH_2), 2855 (v, O−CH_3), 1725 (v, C═O), 1636 (v, C═C), 850−1300 (v, C−C), 1191 (v, C−O).

Using the extraction method in a Soxhlet extractor, the amount of the insoluble fraction of the polymer samples was determined. Polymer samples (0.1 g) were subjected to extraction with acetone for 24 h. The insoluble fraction was dried in a vacuum oven at 20 °C until it reached a consistent mass. The amount of insoluble fraction was estimated by calculating the difference between the initial and final weights following extraction and drying.

The swelling degree of the polymers was determined by using three solvents with different polarities: acetone, toluene, and water. The polymer sample was weighed before being placed into the solvent. Changes in the sample's mass were recorded every 20 min until no further changes were observed.

Tensile strength, Young's modulus, and elongation at break of the polymer samples with dimensions (70 × 10 × 1) ± 0.01 mm were determined by conducting a tensile test using the BDO-FB0.5TH (Zwick/Roell) device. A crosshead speed of 5 mm/min was used. To ensure precision, three measurements were taken to calculate the average value. The experimental results exhibited a variation of no more than 5% within the group.

The glass transition temperature (T_g) of the polymers was determined using an Anton Paar MCR302 rheometer by dynamic

https://doi.org/10.1021/acsapm.5c00412
ACS Appl. Polym. Mater. XXXX, XXX, XXX−XXX

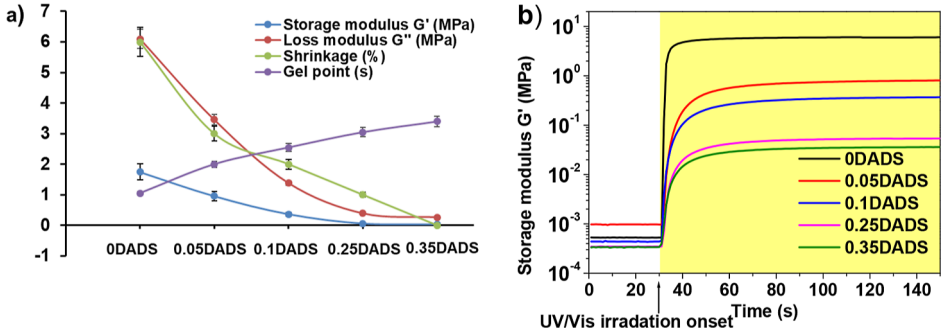

Figure 2. Photorheometric characteristics (a) and storage modulus G' versus time curves (b).

mechanical thermal analysis (DMTA). Samples were tested in shear mode, with the temperature increasing at a rate of 2 °C/min from −30 to 80 °C. The T_g values were identified as the peak maximum of the damping factor (tan δ) curve.

The topology freezing temperature (T_v) was defined using the stress relaxation method with the Anton Paar MCR302 rheometer. Measurements were carried out at 190, 200, 210, and 220 °C for 140 min using a 5% step strain.

The dependence of the change in polymer mass on temperature was determined using the NETZSCH TG 209 thermogravimeter. During the tests, the temperature was increased from 23 to 600 °C. Heating was carried out in a nitrogen atmosphere (with a flow rate of 25 mL/min) at a rate of 10 °C/min. Aluminum oxide crucibles were used for the placement of the samples.

3. RESULTS AND DISCUSSIONS

3.1. Photocuring Kinetics. The study of the photocuring kinetics and rheological properties is important for assessing the potential applications of vitrimers, as it provides information on the curing rate, viscosity, layer shrinkage, and other parameters. The real-time photorheometry allows the behavior of the resin to be understood during the curing process. Investigation of the effect of the amount of DADS on the resin viscosity revealed that, as the amount of DADS increased, the viscosity of the resins decreased. The viscosity of the resin without DADS was 8475 mPa·s, while the viscosity of the resins with the amount of DADS increasing to 0.35 mol gradually decreased (Table 1). The viscosity of the resin with the highest amount of DADS content was 4703 mPa·s and decreased by 55% compared to the resin without DADS, indicating that even very small changes in the DADS content significantly affected the viscosity of the initial mixture. The decrease in viscosity is attributed to the aliphatic structure of DADS and its low molecular weight. The viscosity of the 0.35DADS sample was similar to that of the resin, composed of HPPA, AESO, and MiramerA99, which had a viscosity of 4228 mPa·s and was tested and considered appropriate for digital light processing.[33] The data of the photorheometric characteristics are collected in Figure 2a. The addition of DADS slowed the resin cross-linking, that resulted in a more flexible polymer structure as the gel point values increased and the G' and G'' modulus values decreased by adding up to 0.35 mol of DADS. This happened because the vinyl groups of DADS reacted slower than the acrylic groups of AESO and HPPA,[34] and the aliphatic structure added additional flexibility and softness to the polymer structure. The gel point of a similar resin containing AESO and HPPA was reached in 12 s,[33] while the 0.35DADS resin reached it 4 times faster. Increasing the amount of DADS reduced the shrinkage of the sample layer from 6% to 0%. Low or no shrinkage of the polymer layer is important in the manufacturing of coatings, adhesives, replicas, or 3D printing resins.[35] Figure 2b illustrates the relationship between the G' modulus depending on the duration of UV/vis irradiation. G' is a measure of the elasticity of the material, indicating its ability to store energy. A high G' modulus is characteristic of rigid samples. Irradiation started 30 s after the start of the experiment and continued for 120 s. The G' modulus values started to raise significantly when the resins were exposed to UV/vis radiation. This rapid increase occurred as a result of the polymerization reaction, which started as the polymer chains started to grow, a cross-linked polymer structure formed, and the resin hardened. The softness of the polymer with the higher amount of DADS may be influenced by the decreasing amount of insoluble fraction, since increasing the amount of DADS in the resin left more unreacted functional groups and resulted in a higher quantity of linear and branched soluble oligomers. The induction period was 1 s for all resins. This suggests that the cross-linked structure of the polymer began to form immediately upon exposure to UV/vis radiation.

3.2. Characterization of Cross-Linked Polymer Structure. FT-IR spectroscopy was used to confirm the chemical structure of the synthesized polymers. It was determined that, during photopolymerization, both the acrylic groups of AESO and HPPA, as well as the vinyl groups of AD, reacted. The absorption bands corresponding to these functional groups, observed in the FT-IR spectra of the monomers, decreased but did not completely disappeared. This shows that some of the functional groups remained unreacted because of spatial hindrances typical for cross-linked polymers. In the FT-IR spectrum of DADS presented in Figure S1, a distinct vinyl group peak can be seen at 1636 cm^{-1}, which intensity significantly decreased in the FT-IR spectra of the polymers. To the right of the vinyl group peak, the peaks of the acrylic groups at 1625 cm^{-1} are visible, and their intensity also decreased significantly. The reduction in the peaks of the C═C groups indicates that most of them reacted. Although these two peaks are close in position and partially overlapping, careful analysis allows them to be distinguished. To improve clarity, annotations have been added in Figure S1 to indicate the approximate positions of these overlapping signals. As the DADS content in the resins increased, larger peaks of the C═C groups were observed in the polymer spectra, meaning that more unreacted groups remained in the samples after polymerization. The formation of the polymer was indicated by the broad and merged peaks of the C−C groups in the region of 850−1300 cm^{-1} in the FT-IR spectra of the polymers. Furthermore, the ratio of the characteristic peaks of the acryl and vinyl groups to the reference peak (C═O group)

https://doi.org/10.1021/acsapm.5c00412
ACS Appl. Polym. Mater. XXXX, XXX, XXX−XXX

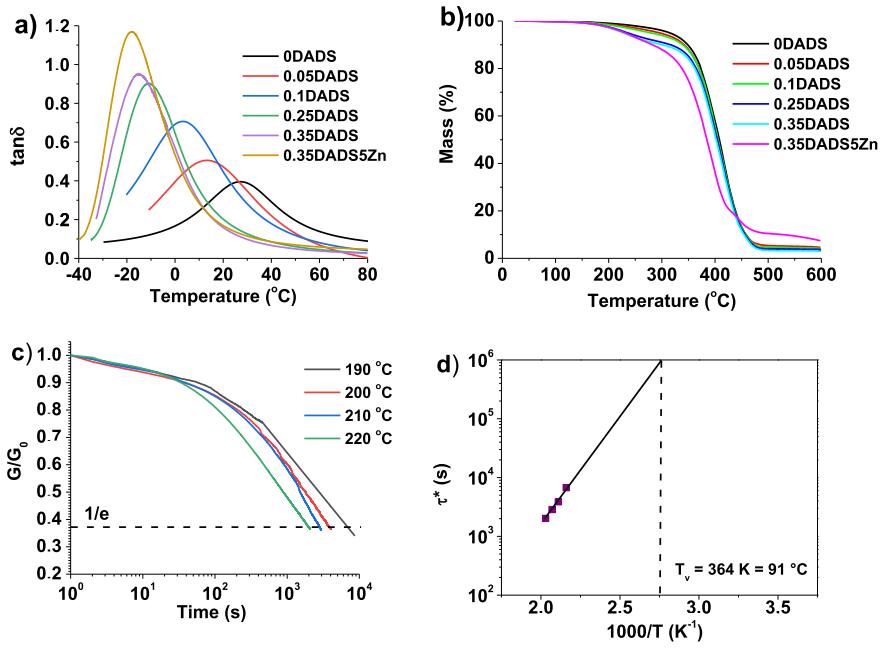

Figure 3. DMTA (a) and thermogravimetric curves (b) of polymers, curves of the time dependence of the stress change of the 0.35DADS5Zn polymer (c), dependence of the duration of the 0.35DADS5Zn stress change of the 0.35DADS5Zn polymer on temperature according to the Arrhenius equation (d).

is proportionally similar. This indicates that both the acrylic groups of AESO and HPPA, as well as the vinyl groups of DADS, reacted during the process.

After extraction with acetone in a Soxhlet extractor, the amount of insoluble fraction, indicating the fraction of the starting materials bonded into the structure of the polymer network, was determined and results are presented in Figure S2. 0DADS polymer had 95% of the insoluble fraction. As the amount of DADS in the resins increased from 0.05 to 0.35 mol, the amount of insoluble fraction of polymers decreased from 91% to 65%. Thus, the 0.35DADS polymer, with the highest amount of DADS had the lowest amount of insoluble fraction (65%). A high amount of soluble fraction indicates that a significant fraction of the monomers and/or oligomers did not integrate into the cross-linked structure. The cross-linking density of the 0DADS polymer, calculated from the G' modulus curves, was 46416 mol/m^3. With the addition of a small amount of DADS, the cross-linking density of the 0.05DADS polymer drastically decreased to 1397 mol/m^3, and for 0.35DADS, it was 109 mol/m^3. The possible reason for this is that the incorporation of DADS fragments increased the size of the network pores.

The swelling of cross-linked polymers can provide insights into their cross-linking degree and the polymer network pore size. In this study, the swelling of polymers was investigated in organic solvents of different polarities (acetone and toluene) and water. The test revealed that the polymers did not swell at all in the nonpolar solvent toluene but swelled in polar solvents, such as acetone and water, because of their affinity. As shown in Figure S3a, the swelling in the water was very low as the DADS content in the samples increased, the swelling degree only changed from 0.33% to 1.4%. The low swelling in the water is probably due to the ability of the oil fragments to repel water. The swelling degree depends on the cross-linking density and the affinity of the polymer to the solvent. The swelling degree in acetone was determined to range from 5% to 59% Figure S3b. As the amount of DADS in the resins increased, swelling of the polymers increased because the pore size increased, and the amount of insoluble fraction decreased. The polymers swelled less in water than in acetone because acetone has a greater affinity for the polymer. Polymers stopped swelling in water after 40 min, while in acetone, 0DADS stopped swelling after 3600 s (60 min), 0.05DADS, 0.1DADS, and 0.25DADS after 4800 s (80 min), and 0.35DADS swelled the longest, up to 6000 s (100 min). The swelling results showed that these polymers are polar and that the polymer network pore size increased while the cross-linking density decreased with the increase of the amount of DADS.

3.3. Thermal Properties. The glass transition temperature (T_g) of the polymers was determined using dynamic mechanical thermal analysis (DMTA), and thermogravimetric analysis (TGA) was used to identify their thermal stability. These parameters are particularly valuable for the application and polymer reprocessing. When the amount of DADS in the resins increased, the T_g of the polymers decreased as can be seen in Figure 3a. According to the highest values of the tan δ curves, the T_g of the 0DADS polymer was 30 °C, while for 0.35DADS it was −15 °C. The T_g of the polymer with the catalyst, 0.35DADS5Zn, was the lowest (−18 °C). The lengthening of the aliphatic chains in the polymers was the reason for the decrease in T_g, the decrease in the cross-linking density, and the reduction in the insoluble fraction, which was determined by extracting the samples with acetone. Despite the low T_g, the polymer samples were not liquid at room temperature but formed soft films, which is common for cross-linked polymers that have long aliphatic chains.[36]

The thermal decomposition temperature of the polymers at 5% weight loss ($T_{dec.-5\%}$) was determined by TGA and the TGA curves are shown in Figure 3b. As the DADS amount increased, the thermal stability of the polymers decreased from 315 to 236 °C, due to the lengthening of the aliphatic chains,

https://doi.org/10.1021/acsapm.5c00412
ACS Appl. Polym. Mater. XXXX, XXX, XXX−XXX

the reduced cross-linking density, and the decrease in the amount of insoluble fraction. The addition of a catalyst accelerated thermal degradation and increased the residue. The $T_{dec.-5\%}$ of the synthesized polymers was higher than that of a starch-based polymer with disulfide bonds ($T_{dec.-5\%}$ = 231 °C).[37] All polymers synthesized in this study were thermally stable up to 200 °C.

The topology freezing temperature (T_v) is a valuable parameter of vitrimers with dynamic covalent bonds that can be thermally reprocessed into new materials. Below T_g, vitrimers behave like thermosets, while above T_v, they act like thermoplastics because at that temperature, the covalent bonds break down and new covalent bonds form. T_v is the upper limit for vitrimer operation and the lowest temperature for reprocessing. In this study, the polymer T_v value was estimated through stress relaxation tests on samples. The relaxation time (τ^*) of the 0.35DADS5Zn polymer, which was chosen for the experiment due to the highest number of dynamic bonds and the presence of a catalyst that activates the reactions, was determined at different temperatures, below the thermal decomposition temperature, but above T_v. As the temperature increased, dynamic disulfide bond exchange occurred, leading to a reduction in τ^* from 2.4 h to 35 min as presented in Figure 3c. The T_v of the 0.35DADS5Zn polymer, determined by extrapolating the results using the Arrhenius equation as demonstrated in Figure 3d, is 91 °C. Since the 0.35DADS5Zn sample has a T_v, this polymer can be classified as a vitrimer.

3.4. Mechanical Properties. The mechanical properties of the vitrimer samples were investigated through tensile testing. The mechanical characteristics, including tensile strength, Young's modulus, and elongation at break are summarized in Table 2. The 0DADS sample exhibited the highest tensile strength of 11.33 ± 0.65 MPa. The tensile strength of the 0.05DADS sample decreased 2.5 times and that of 0.35DADS decreased by 14 times. The elongation at break values increased with the amount of DADS, ranging from 33.48% to 62%. Young's modulus in the sample without DADS (0DADS) reached 65.6 MPa, but after adding 0.05 mol of DADS, it drastically decreased to 2.14 MPa for the 0.05DADS sample and to 0.12 MPa for the 0.35DADS sample. When a catalyst was added to the sample, the mechanical properties of the 0.35DADS5Zn sample changed little: the tensile strength was 0.31 MPa, the elastic modulus was 0.23 MPa, and the elongation at break increased by 6%. Higher DADS amount caused weaker mechanical properties because, in samples with more fragments of DADS, the aliphatic chains lengthened, the cross-linking density decreased, and there was less insoluble fraction, making the polymer softer and more flexible.

Table 2. Mechanical Characteristics of Polymers

polymer	tensile strength (MPa)	elongation at break (%)	Young's modulus (MPa)
0DADS	11.33 ± 0.65	33.48 ± 6.50	65.60 ± 10.00
0.05DADS	4.42 ± 0.20	44.08 ± 5.0	2.14 ± 0.54
0.1DADS	1.55 ± 0.15	58.72 ± 8.30	0.62 ± 0.02
0.25DADS	1.05 ± 0.20	60.00 ± 4.60	0.16 ± 0.06
0.35DADS	0.80 ± 0.10	62.00 ± 11.50	0.12 ± 0.01
0.35DADS5Zn	0.31 ± 0.08	56.03 ± 7.70	0.23 ± 0.02

3.5. Self-Welding Properties. The self-welding of polymers is beneficial because it extends the life of the product, reduces plastic waste, and lowers production costs. The study of self-welding properties was carried out on a sample with the highest DADS concentration (0.35 mol) and an additional 5 wt % of catalyst. The catalyst was added to accelerate the reversible exchange of covalent bonds. The two halves of the cut polymer sample were placed on top of each other, pressed manually, and heated at 180 °C for 1 h. The sample was heated at a temperature higher than T_v because this activates the disulfide bond exchange reactions. After 1 h of heating, the polymer sample was welded: the joined parts adhered to each other, as shown in Figure 4a, due to the exchange of covalent bonds between the cut parts of the sample. A tensile testing was carried out and the results demonstrated that the heated and welded sample had greater elongation at break (68.75 ± 1.68%) compared to the original sample (56.03 ± 7.70%). Tensile strength remained almost unchanged (0.29 ± 0.06 MPa), while Young's modulus decreased 4.5 times (0.05 ± 0.01 MPa). The self-welding efficiency, calculated as the ratio of the tensile strength of the welded sample and the original sample, was 94%. This polymer exhibited self-welding properties due to dynamic bond exchanges, allowing the damaged sample to be repaired.

3.6. Shape-Memory Properties. The shape memory of polymer allows a polymer product to regain its permanent shape after deformation. This feature is particularly valuable in microimprint lithography applications, such as creating precise patterns for flexible electronics, optical components, and microfluidic devices, where accuracy ensuring optimal functionality and durability giving consistent performance under repeated use are essential. The thermal response of the shape memory properties of the 0.35DADS5Zn polymer sample was studied by deforming it to a temporary spiral shape at room temperature. The temporary shape was stabilized by lowering the temperature below T_g (5 °C) of the sample. The sample was brought back to room temperature to allow the temporary shape to regain its permanent shape. Photos of the sample returning to its permanent shape are shown in Figure 4b. It can be seen that after 30 s the sample had just begun to unwind, after 60 s it was halfway through the

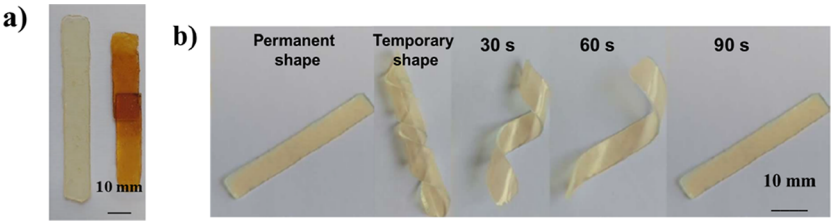

Figure 4. Images of the 0.35DADS5Zn polymer sample: top image—original sample, before self-welding, bottom image—after self-welding (a) and photos of the 0.35DADS5Zn polymer sample during return to its permanent shape (b).

https://doi.org/10.1021/acsapm.5c00412
ACS Appl. Polym. Mater. XXXX, XXX, XXX−XXX

process, and after 90 s it had completely returned to its permanent shape. The sample demonstrated the ability to undergo such shape transitions repeatedly, indicating that the process can be carried out an unlimited number of times under the given conditions.

3.7. Reprocessability of Polymers. The reprocessability of polymers demonstrates whether a polymer can be reused and recycled multiple times, thereby preventing the accumulation of large amounts of polymer waste. In addition, reprocessability helps to reduce production costs as recycling waste decreases the need for new raw materials. As shown in Figure S4, the 0.35DADS5Zn polymer sample was recycled by grinding it into powder, and the resulting powder was pressed at a temperature above its T_v. The individual polymer powder particles fused into a continuous product, a film, due to disulfide bond exchanges. A tensile testing results demonstrated that reprocessed sample had lower elongation at break (2.90 ± 0.51%) compared to the original sample (56.03 ± 7.70%). This indicates that the reprocessing process significantly reduced the ability to stretch before breaking. The tensile strength, however, remained nearly unchanged at 0.19 ± 0.01 MPa, suggesting that the reprocessing did not affect the resistance to force. On the other hand, Young's modulus increased by 12 times, from 0.24 ± 0.02 to 2.84 ± 0.28 MPa, showing that the sample became significantly stiffer due to the structural changes. Furthermore, the intensities of the OH and C═O group signals at 3495 and 1744 cm^{-1}, respectively, in the FT-IR spectrum after reprocessing were identical to those of the original samples (Figure S5). This shows that further polymerization of unreacted monomers upon heating did not occur and the sample was reprocessed due to the dynamic reactions. Synthesized vitrimer can be recycled from its waste materials, as demonstrated in the reprocessability experiment.

3.8. Antimicrobial Properties. The antibacterial and antifungal activity of the polymer films was evaluated after 1 h of direct contact of the bacterial or fungal suspensions with the specimens and the results are shown in Figure 5. Polymer

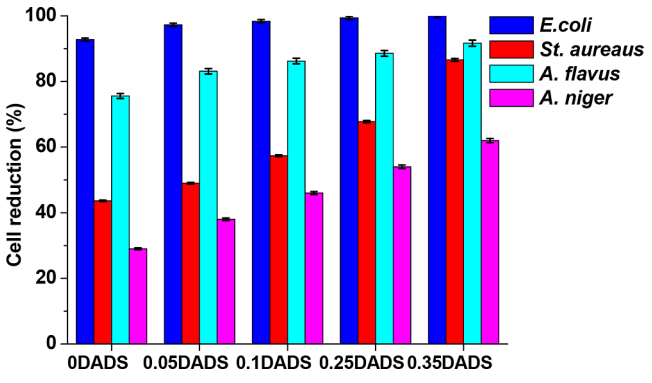

Figure 5. Cell reduction of *E. coli*, *S. aureus*, *A. flavus* and *A. niger* after 1 h of direct contact of polymer samples with bacterial and fungal suspensions.

sample without DADS showed antimicrobial activity as the hydroxyl and carbonyl groups can contribute to the antimicrobial effect.[38] Even 0.05 mol of DADS had an effect on microbial growth, and by increasing the DADS concentration, the cell reduction increased for all microorganisms showing that a higher amount of DADS led to more significant antimicrobial or antifungal activity. Sample 0.35DADS demonstrated the highest effectiveness against *E. coli* with a 100% cell reduction and this value was higher compared to vitrimers with typical antimicrobial components, such as alkyl-substituted quaternary ammonium groups (95%).[39] While *S. aureus* was less sensitive than *E. coli* with 87% cell reduction of sample 0.35DADS. The highest cell reduction against *A. flavus* was 92%. DADS had the least impact on *A. niger* resulting in the lowest cell reduction with all amounts of DADS. The antimicrobial activity of polymers with DADS fragments increased because DADS can damage bacterial cell membranes, leading to leakage of vital intracellular components and death.[40] DADS can bind to proteins-containing thiol groups and generate disulfide band, resulting in protein denaturation.[41] In addition, DADS can disrupt the quorum sensing system which is used to communicate and regulate gene expression based on their population density.[42] The results of antimicrobial activity highlight the potential of vitrimers containing DADS fragments as effective antimicrobial films or microstructures.

3.9. Microimprint Lithography Testing. The 0.35DADS resin was tested in a high-precision microimprint lithography technique to fabricate microscale patterns. Images captured during the testing are presented in Figure 6. The resin replica

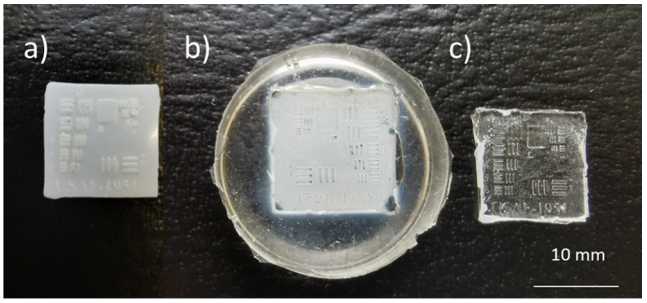

Figure 6. Images captured during the trial using microimprint lithography: a 3D printed 1951 USAF target (a), a PDMS mold (b), and a replica produced from 0.35DADS resin (c).

accurately replicated the shape and features of the PDMS mold, including the letters and numbers. The line widths achieved ranged from 69 ± 0 μm to approximately 220−230 ± 5 μm. The replica exhibited only minor imperfections, such as slight rounding of edges caused by peeling of the stamp. The optimized viscosity allowed a uniform resin distribution on the PDMS mold, ensuring a consistent patterning without defects. Additionally, the controlled process of photocuring kinetics ensured that the resin cured at a rate that minimized shrinkage and deformation, which are critical factors in the fabrication of microstructures. The flexibility of the polymers imparted by DADS contributed to the smooth release of the mold after photocuring. The ability of 0.35DADS resin to produce highly accurate microstructures makes it an excellent candidate for various microimprint lithography applications where precision is required, including microelectronic devices and biosensors.

4. CONCLUSIONS

The influence of the amount of diallyl disulfide on the properties of biobased vitrimers synthesized from acrylated epoxidized soybean oil, 2-hydroxy-3-phenoxypropyl acrylate, and diallyl disulfide was determined. Increasing the amount of diallyl disulfide reduced viscosity and shrinkage, improved flexibility, making vitrimers suitable for advanced applications such as microimprint lithography. The polymers showed self-

https://doi.org/10.1021/acsapm.5c00412
ACS Appl. Polym. Mater. XXXX, XXX, XXX−XXX

welding with 94% efficiency and shape-memory properties, enabled by dynamic disulfide bond exchanges. Importantly, antimicrobial tests demonstrated significant activity against bacteria and fungi, particularly with higher amounts of diallyl disulfide. 100% activity against *E. coli* was reached even after 1 h of direct contact of the bacterial suspension (1.75×10^6 colony forming units/mL) with the polymer samples. The successful application of the resin in microimprint lithography demonstrated its potential in high-precision patterning. The resin achieved accurate replication of fine microstructures, highlighting possible suitability for fabricating microscale components used in microelectronic devices, biosensors, and optical systems. The exceptional properties of diallyl disulfide-based polymers make them versatile materials for industrial and engineering applications.

■ ASSOCIATED CONTENT

Supporting Information

The Supporting Information is available free of charge at https://pubs.acs.org/doi/10.1021/acsapm.5c00412.

FT-IR spectra of AESO, HPPA, DADS, and their polymers; yield of the insoluble fraction and cross-linking density of polymers; dependence of the degree of polymer swelling on swelling duration in water and acetone; reprocessing photos of the 0.35DADS5Zn polymer sample; FT-IR spectra before and after reprocessing (PDF)

■ AUTHOR INFORMATION

Corresponding Author

Jolita Ostrauskaite − *Department of Polymer Chemistry and Technology, Kaunas University of Technology, LT-50254 Kaunas, Lithuania;* orcid.org/0000-0001-8600-7040; Email: jolita.ostrauskaite@ktu.lt

Authors

Liepa Daugelaite − *Department of Polymer Chemistry and Technology, Kaunas University of Technology, LT-50254 Kaunas, Lithuania*

Sigita Grauzeliene − *Department of Polymer Chemistry and Technology, Kaunas University of Technology, LT-50254 Kaunas, Lithuania;* orcid.org/0000-0003-1953-1074

Danguole Bridziuviene − *Biodeterioration Research Laboratory, Nature Research Center, LT-08412 Vilnius, Lithuania*

Vita Raudoniene − *Biodeterioration Research Laboratory, Nature Research Center, LT-08412 Vilnius, Lithuania*

Egidija Rainosalo − *Centria University of Applied Sciences, FI-67100 Kokkola, Finland*

Complete contact information is available at: https://pubs.acs.org/10.1021/acsapm.5c00412

Funding

This research was funded by the Research Council of Lithuania (project no. S-MIP-23−52).

Notes

The authors declare no competing financial interest.

■ ACKNOWLEDGMENTS

The Chemistry and Bioeconomy team at the Centria University of Applied Sciences is gratefully acknowledged for their invaluable support, including guidance on materials testing and access to equipment. Prof. dr. M. Malinauskas and dr. E. Skliutas from the Laser Research Center, Faculty of Physics, Vilnius University, are sincerely acknowledged for providing the 3D-printed target used in the microimprint lithography test.

■ REFERENCES

(1) Alkarri, S.; Bin Saad, H.; Soliman, M. On antimicrobial polymers: development, mechanism of action, international testing procedures, and applications. *Polymers* **2024**, *16* (6), 771.

(2) Wi, Y. M.; Patel, R. Understanding biofilms and novel approaches to the diagnosis, prevention, and treatment of medical device-associated infections. *Infect. Dis. Clin.* **2018**, *32* (4), 915−929.

(3) Kouhi, M.; Prabhakaran, M. P.; Ramakrishna, S. Edible polymers: An insight into its application in food, biomedicine and cosmetics. *Trends Food Sci. Technol.* **2020**, *103*, 248−263.

(4) Makvandi, P.; Iftekhar, S.; Pizzetti, F.; Zarepour, A.; Zare, E. N.; Ashrafizadeh, M.; Agarwal, T.; Padil, V. V. T.; Mohammadinejad, R.; Sillanpaa, M.; et al. Functionalization of polymers and nanomaterials for water treatment, food packaging, textile and biomedical applications: a review. *Environ. Chem. Lett.* **2021**, *19*, 583−611.

(5) Chua, M. H.; Cheng, W.; Goh, S. S.; Kong, J.; Li, B.; Lim, J. Y.; Loh, X. J. Face masks in the new COVID-19 normal: materials, testing, and perspectives. *Research* **2020**, *2020*, 7286735.

(6) Fatima, S. N. Microbial Biopolymers: A Sustainable Alternative to Traditional Petroleum-Based Polymers for a Greener Future. *Mater. Today Commun.* **2024**, *40*, 109846.

(7) Muñoz-Bonilla, A.; Echeverria, C.; Sonseca, A.; Arrieta, M. P.; Fernández-García, M. Bio-based polymers with antimicrobial properties towards sustainable development. *Materials* **2019**, *12* (4), 641.

(8) Liu, Y.; Wang, S.; Dong, J.; Huo, P.; Zhang, D.; Han, S.; Yang, J.; Jiang, Z. External Stimuli-Induced Welding of Dynamic Cross-Linked Polymer Networks. *Polymers* **2024**, *16* (5), 621.

(9) Kasemsiri, P.; Lorwanishpaisarn, N.; Pongsa, U.; Ando, S. Reconfigurable shape memory and self-welding properties of epoxy phenolic novolac/cashew nut shell liquid composites reinforced with carbon nanotubes. *Polymers* **2018**, *10* (5), 482.

(10) Krishnakumar, B.; Sanka, R. V. S. P.; Binder, W. H.; Parthasarthy, V.; Rana, S.; Karak, N. Vitrimers Associative dynamic covalent adaptive networks in thermoset polymers. *Chem. Eng. J.* **2020**, *385*, 123820.

(11) Guerre, M.; Taplan, C.; Winne, J. M.; Du Prez, F. E. Vitrimers: directing chemical reactivity to control material properties. *Chem. Sci.* **2020**, *11* (19), 4855−4870.

(12) Alabiso, W.; Schlögl, S. The impact of vitrimers on the industry of the future: Chemistry, properties and sustainable forward-looking applications. *Polymers* **2020**, *12* (8), 1660.

(13) Rekondo, A.; Martin, R.; Ruiz de Luzuriaga, A.; Cabañero, G.; Grande, H. J.; Odriozola, I. Catalyst-free room-temperature self-healing elastomers based on aromatic disulfide metathesis. *Mater. Horiz.* **2014**, *1* (2), 237−240.

(14) Guo, X.; Liu, F.; Lv, M.; Chen, F.; Gao, F.; Xiong, Z.; Chen, X.; Shen, L.; Lin, F.; Gao, X. Self-healable covalently adaptable networks based on disulfide exchange. *Polymers* **2022**, *14* (19), 3953.

(15) Sahu, S.; Niranjan, R.; Priyadarshini, R.; Lochab, B. Benzoxazine-grafted-chitosan biopolymer films with inherent disulfide linkage: Antimicrobial properties. *Chemosphere* **2023**, *328*, 138587.

(16) Porcarello, M.; Mendes-Felipe, C.; Lanceros-Mendez, S.; Sangermano, M. Design of acrylated epoxidized soybean oil biobased photo-curable formulations for 3D printing. *Sustainable Mater. Technol.* **2024**, *40*, No. e00927.

(17) Lascano, D.; Gomez-Caturla, J.; Garcia-Sanoguera, D.; Garcia-Garcia, D.; Ivorra-Martinez, J. Optimizing biobased thermoset resins by incorporating cinnamon derivative into acrylated epoxidized soybean oil. *Mater. Des.* **2024**, *243*, 113084.

(18) Bodor, M.; Lasagabáster-Latorre, A.; Arias-Ferreiro, G.; Dopico-García, M. S.; Abad, M. J. Improving the 3D Printability

and Mechanical Performance of Biorenewable Soybean Oil-Based Photocurable Resins. *Polymers* **2024**, *16* (7), 977.
(19) Moazzen, K.; Rossegger, E.; Alabiso, W.; Shaukat, U.; Schlögl, S. Role of Organic Phosphates and Phosphonates in Catalyzing Dynamic Exchange Reactions in Thiol-Click Vitrimers. *Macromol. Chem. Phys.* **2021**, *222*, 2100072.
(20) Rossegger, E.; Höller, R.; Reisinger, D.; Strasser, J.; Fleisch, M.; Griesser, T.; Schlögl, S. Digital Light Processing 3D Printing with Thiol−Acrylate Vitrimers. *Polym. Chem.* **2021**, *12*, 639−644.
(21) Li, H.; Zhang, B.; Wang, R.; Yang, X.; He, X.; Ye, H.; Cheng, J.; Yuan, C.; Zhang, Y. F.; Ge, Q. Solvent-Free Upcycling Vitrimers through Digital Light Processing-Based 3D Printing and Bond Exchange Reaction. *Adv. Funct. Mater.* **2022**, *32*, 2111030.
(22) Nakamoto, M.; Kunimura, K.; Suzuki, J. I.; Kodera, Y. Antimicrobial Properties of Hydrophobic Compounds in Garlic: Allicin, Vinyldithiin, Ajoene and Diallyl Polysulfides. *Exp. Ther. Med.* **2019**, *19* (2), 1550−1553.
(23) Xue, H.; Ding, X.; Zhang, Y.; Li, X.; Xia, J.; Lin, Q. Disulfide Group Influence on the Surface Properties and Reversible Cross-Linking Functionalization of Natural Polymer Coating. *Polym. Bull.* **2021**, *78*, 6707−6721.
(24) Sonaji, A. V.; Pradeep, A. R.; Ganesh, C. S.; Sambhaji, D. G.; Kumar, R.; Kumar, R.; Mziray, A. N.; Boateng, E. A.; Nyarko, R. O.; Boateng, P. O. Biological Benefits of Diallyl Disulfide, a Garlic-Derived Natural Organic Sulfur Compound. *IJRASB* **2024**, *3* (1), 147−153.
(25) Green, W. A. *Industrial Photoinitiators: A Technical Guide*; CRC Press, 2010.
(26) Liu, T.; Zhao, B.; Zhang, J. Recent Development of Repairable, Malleable and Recyclable Thermosetting Polymers through Dynamic Transesterification. *Polymer* **2020**, *194*, 122392.
(27) Unno, N.; Mäkelä, T. Thermal Nanoimprint Lithography—A Review of the Process, Mold Fabrication, and Material. *Nanomaterials* **2023**, *13* (14), 2031.
(28) Lebedevaite, M.; Ostrauskaite, J. Influence of photoinitiator and temperature on photocross-linking kinetics of acrylated epoxidized soybean oil and properties of the resulting polymers. *Ind. Crops Prod.* **2021**, *161*, 113210.
(29) Grauzeliene, S.; Kastanauskas, M.; Talacka, V.; Ostrauskaite, J. Photocurable glycerol-and vanillin-based resins for the synthesis of vitrimers. *ACS Appl. Polym. Mater.* **2022**, *4* (8), 6103−6110.
(30) Kazlauskaite, B.; Grauželienė, S.; Bridziuviene, D.; Raudoniene, V.; Rainosalo, E.; Ostrauskaite, J. Antimicrobial thiol-acrylate vitrimers synthesized from glycerol and vanillin derivatives. *Smart Mater. Struct.* **2025**, *34*, 035044.
(31) Navaruckiene, A.; Bridziuviene, D.; Raudoniene, V.; Rainosalo, E.; Ostrauskaite, J. Vanillin Acrylate-Based Thermo-Responsive Shape Memory Antimicrobial Photopolymers. *eXPRESS Polym. Lett.* **2022**, *16* (3), 279−295.
(32) Flory, P. J. *Principles of Polymer Chemistry*; Cornell University Press, 1953.
(33) Grauzeliene, S.; Schuller, A. S.; Delaite, C.; Ostrauskaite, J. Biobased Vitrimer Synthesized from 2-Hydroxy-3-Phenoxypropyl Acrylate, Tetrahydrofurfuryl Methacrylate and Acrylated Epoxidized Soybean Oil for Digital Light Processing 3D Printing. *Eur. Polym. J.* **2023**, *198*, 112424.
(34) Lee, T. Y.; Roper, T. M.; Jonsson, E. S.; Kudyakov, I.; Viswanathan, K.; Nason, C.; Guymon, C. a.; Hoyle, C. The Kinetics of Vinyl Acrylate Photopolymerization. *Polymer* **2003**, *44* (10), 2859−2865.
(35) Luck, R. M.; Sadhir, R. K. Shrinkage in Conventional Monomers during Polymerization. In *Expanding Monomers*; CRC Press, 2020; pp 1−20.
(36) Yang, Q.; Li, W.; Stober, S. T.; Burns, A. B.; Gopinadhan, M.; Martini, A. Effect of Aliphatic Chain Length on the Stress−Strain Response of Semiaromatic Polyamide Crystals. *Macromolecules* **2022**, *55* (12), 5071−5079.
(37) Tratnik, N.; Tanguy, N. R.; Yan, N. Recyclable, Self-Strengthening Starch-Based Epoxy Vitrimer Facilitated by Exchangeable Disulfide Bonds. *J. Chem. Eng.* **2023**, *451*, 138610.
(38) Olmos, D.; González-Benito, J. Polymeric Materials with Antibacterial Activity: A Review. *Polymers* **2021**, *13* (4), 613.
(39) Yang, Y.; Xia, Z.; Huang, L.; Wu, R.; Niu, Z.; Fan, W.; Dai, Q.; He, J.; Bai, C. Renewable Vanillin-Based Thermoplastic Polybutadiene Rubber: High Strength, Recyclability, Self-Welding, Shape Memory, and Antibacterial Properties. *ACS Appl. Mater. Interfaces* **2022**, *14* (41), 47025−47035.
(40) Manjhi, M. K.; Chauhan, P.; Upadhyaya, C. P.; Singh, A. K.; Anupam, R. Mechanism of Antibacterial Activity of Diallyl Sulfide against Bacillus cereus. *J. Ayurveda Integr. Med.* **2024**, *15*, 100951.
(41) Feng, S.; Eucker, T. P.; Holly, M. K.; Konkel, M. E.; Lu, X.; Wang, S. Investigating the Responses of Cronobacter sakazakii to Garlic-Derived Organosulfur Compounds. *Appl. Environ. Microbiol.* **2014**, *80* (3), 959−971.
(42) Li, W. R.; Ma, Y. K.; Xie, X. B.; Shi, Q. S.; Wen, X.; Sun, T. L.; Peng, H. Diallyl Disulfide from Garlic Oil Inhibits Pseudomonas aeruginosa Quorum Sensing Systems. *Front. Microbiol.* **2019**, *9*, 3222.

https://doi.org/10.1021/acsapm.5c00412
ACS Appl. Polym. Mater. XXXX, XXX, XXX−XXX